VEX1 controls the allelic exclusion required for antigenic variation in trypanosomes

Lucy Glover, Sebastian Hutchinson, Sam Alsford and David Horn

Supporting Information Appendix

Materials and Methods

T. brucei growth and manipulation

Bloodstream-form *T. brucei*, Lister 427 and 2T1 cells (1) were grown in HMI-11 medium and genetically manipulated using electroporation as described (2); cytomix was used for all transfections other than for RNAi library generation. The subtelomeric *NPT*-reporter cassette within 2-kbp of a *de-novo* telomere was derived from pTMF (3). Assembly of the bloodstream-form *T. brucei* RNAi library was carried out as described (2) and the library incorporating the *NPT*-reporter was grown under RNAi-inducing conditions (tetracycline, Tet at 1 $\mu g.ml^{-1}$) 24 h prior to G418-selection at 50 $\mu g.ml^{-1}$ for 12 days. Puromycin, phleomycin, hygromycin and blasticidin were used at 2, 2, 2 and 10 $\mu g.ml^{-1}$ for selection of recombinant clones; and at 1, 1, 1 and 2 $\mu g.ml^{-1}$, respectively, for maintaining those clones. Exceptions were G418 used at 1 $\mu g.ml^{-1}$ to select for integration of the *GFP:NPT* bicistron with common UTRs and at 250 $\mu g.ml^{-1}$ over 10 days to select for *VSG-5/NPT* co-activation, starting with 1.5 x 10^6 cells. In the latter case, cells that were >99% VSG-5 negative, as determined by immunofluorescence microscopy, were sub-cloned prior to selection. Cumulative growth curves were generated from cultures seeded at 10^5 $cells.ml^{-1}$, counted on a haemocytometer and diluted back to below 10^5 $cells.ml^{-1}$ as necessary. Established procyclic-form *T. brucei*, Lister 427 cells were grown in SDM-79 at 27°C and genetically manipulated by electroporation using 10 μg linearized DNA in a 4-mm gap cuvette and a Gene Pulser (Bio-Rad) set at 1.4-kV, 400-Ω and 25-µF. Electroporated cells were selected in 96-well plates after 24 h; hygromycin and blasticidin were used at 25 and 50 $\mu g.ml^{-1}$, respectively.

Plasmids

Specific RNAi target fragments of 574 bp (Tb927.11.16920) or 418 bp (Tb927.6.4330) were amplified using PCR primers designed using RNAit (4) and cloned into $pRPa^{iSL}$ (5). For epitope-tagging at native loci, fragments of 915 bp (Tb927.11.16920) or 1069 bp

(Tb927.6.4330) were amplified and cloned in pNAT^{xTAG} (5) to add a 12 x c-myc *C*-terminal epitope tag. An 1146 bp fragment of TRF2 (Tb927.10.12850) was amplified and cloned in pNAT^{TAGx} to add an *N*-terminal GFP-tag. For overexpression, the 2754 bp open reading-frame of Tb927.11.16920 was amplified and cloned in the pRPa^{ix6mycx} vector with or without fusion to a *C*-terminal myc-tag. RNAi-knockdown constructs under the control of tetracycline-inducible promoters were targeted to a single genomic locus validated for robust expression, and GFP or c-myc based vectors were used to add fluorescent or epitope-tags to native gene loci (5). Reporter strains were generated using telomere-mediated chromosome-fragmentation with derivatives of pTMF (3). The *VSG-5* reporter, p5^{N}TMF, was constructed by replacing the *VSG-2* associated sequence with an *rDNA* promoter and a *VSG-5* ORF with a *procyclin* 5'-sequence and *VSG-2* 3'-sequence. The latter sequence incorporates 77 bp up to the polyadenylation site and 819 bp beyond this site. The bicistronic reporter with common UTRs, pGFP^{NAA}TMF, was constructed by replacing the *VSG-2* associated sequence with an *rDNA* promoter and *GFP* ORF with a *procyclin* 5'-sequence and *aldolase* 3'-sequence. The latter sequence incorporates 651 bp up to the polyadenylation site and 70 bp beyond this site. The bicistronic reporter with distinct UTRs, pGFP^{NTA}TMF, was constructed by replacing the *GFP*-associated *aldolase* 3'-sequence with a *tubulin* 3'-sequence. Oligonucleotide sequences are available on request.

Nucleic acid analysis

RIT-seq was carried out on a MiSeq platform (Illumina) at BGI (The Beijing Genome Institute) and reads were mapped to the *T. brucei* 927 reference genome (v6, tritrypdb.org) with Bowtie 2 (6) using the parameters --very-sensitive-local --phred33. Alignment files were manipulated with SAMtools (7) and a custom-script (2) and data were further assessed using the Artemis genome browser (8); 518,000 mapped reads. For RNA-seq, we used pairs of wild-type clones and pairs of strains, either uninduced or induced for VEX1 overexpression or knockdown for 72 h; population density was reduced by 74% and 24%, respectively,

following induction for 72 h. Briefly, polyadenylated transcripts were enriched using poly-dT beads and reverse-transcribed before sequencing on a HiSeq platform (Illumina) at the University of Dundee or at BGI. Reads were mapped to a hybrid genome assembly consisting of the *T. brucei* 927 reference genome plus the bloodstream *VSG*-ESs (9) and metacyclic *VSG*-ESs (10, 11) from the Lister 427 strain used in this study. Bowtie 2-mapping was with the parameters --very-sensitive --no-discordant --phred33. Alignment files were manipulated with SAMtools (7). Per-gene read counts were derived using the Artemis genome browser (8); MapQ, 0. Read counts were normalised using edgeR and differential expression was determined with classic edgeR. RPKM values were derived from normalised read counts in edgeR (12). Southern blotting and Northern blotting were carried out according to standard protocols.

Western blotting

Western blotting was carried out according to standard protocols. Rabbit α-VSG-2, rabbit α-VSG-5 and rabbit α-VSG-6 were all used at 1:20,000, while mouse α-myc (Source Bioscience) was used at 1:2,000. Blots were developed using an enhanced chemiluminescence kit (Amersham) according to the manufacturer's instructions.

Microscopy

Immunofluorescence microscopy was carried out according to standard protocols, typically using wild-type cells and cells induced for VEX1 knockdown or overexpression for 72 h. We used 'antigen-retrieval' for quantitative analysis of pol-I and VEX1 and for 3D-SIM. In these cases, prior to permeabilization, fixed cells were rehydrated in PBS for 5 min at RT, held at 95°C for 60 s in antigen retrieval buffer (100 mM Tris, 5% urea, pH 9.5) and then washed 3 x 5 min in PBS at RT. Primary antisera were rat α-VSG-2 (1:10,000), rabbit α-VSG-5 (1:10,000), rabbit α-VSG-6 (1:10,000), rabbit α-GFP (1:500, Invitrogen), mouse α-myc (1:400, Source Bioscience) and rabbit α–NOG1 (1:500, Tb927.11.3120) (13). α–pol-1

antisera (1:200) were raised in rabbits against two peptides (DTAILRDVLERNFA and DTGGPQRRRGSVESGRGD - Tb927.8.5090; Perbio). Cells were mounted in Vectashield (Vector Laboratories) containing DAPI (4',6-diamidino-2-phenylindole). For standard immunofluorescence microscopy, secondary antibodies (Pierce) were FITC conjugated α-rabbit (1:2000), FITC-conjugated α-mouse (1:2000) and rhodamine conjugated α-rat (1:2000). In *T. brucei*, DAPI-stained nuclear and mitochondria DNA can be used as cytological markers for cell-cycle stage; one nucleus and one kinetoplast (1N:1K) indicates G_1, one nucleus and an elongated kinetoplast (1N:eK) indicates S-phase, one nucleus and two kinetoplasts (1N:2K) indicates G_2/M and two nuclei and two kinetoplasts (2N:2K) indicates post-mitosis. We used an Eclipse E600 epifluorescence (Nikon) or a Zeiss Axiovert 200M microscope. Images were captured using a Coolsnap FX (Photometrics) CCD, or a AxioCam MRm camera, respectively. Images were processed using Metamorph and analyzed using ImageJ. Actinomycin D was applied at 10 $\mu g.ml^{-1}$ and eliminated focal VEX1 signals, detectable in >60% of control cell nuclei. For 3D-SIM, secondary Alexa Fluor conjugated goat antibodies (ThermoFisher) were α-rabbit 488, α-rat 647 and α-mouse 568, all used at 1 $\mu g.ml^{-1}$. These cells were mounted on precision cover glass (Marienfeld; thickness N^o. 1.5H, tol. +/- 5 μm) and analyzed using a super-resolution OMX Blaze system (GE Healthcare).

Flow cytometry

Fluorescence activated cell sorting was carried out according to standard protocols. Briefly, VSGs were detected using rat α-VSG-2 (1:10,000) and rabbit α-VSG-6 (1:10,000) primary antibodies. Secondary antibodies were goat α-rat Alexa Fluor 647 and goat α-rabbit Alexa Fluor 488 both at $1\mu g.ml^{-1}$. DNA was stained with propidium iodide at 5 $\mu g.ml^{-1}$. Samples were analyzed on a FACS Canto (Becton Dickinson) and data were visualized using FlowJo software.

Quantitative mass spectrometry

GPI-specific phospholipase C (GPI-PLC) cleaved soluble VSG (sVSG) was prepared as described (14), except the eluate was concentrated on an Amicon Ultra 0.5 ml centrifugal filter (Millipore), and recovered in 100 µl of water. We used wild-type cells and cells induced for VEX1 knockdown or overexpression for 72 h. sVSG samples at 0.5 $\mu g.\mu l^{-1}$ in 50 mM ammonium bicarbonate and 0.5% RapiGest SF (Waters Corp., USA) were reduced in 10 mM DTT (Calbiochem, Clelands Reagent, ULTROL Grade) at 56˚C for 1 h and alkylated with 50 mM iodoacetamide for 30 min at 20˚C. Trypsin-digestion (Pierce, 0.25 µg MS-Grade Trypsin) was in a ThermoMixer (Eppendorf) for 16 h at 30˚C and 900 rpm. Samples were then adjusted to 1% formic acid and incubated for 45 m at 37˚C and 900 rpm. Samples were spun for 10 min at 14,500 rpm and injected (10 µl) into an Ultimate 3000 RSLCnano system (Thermo Scientific) coupled to a Linear Trap Quadropole OrbiTrap Velos Pro (Thermo Scientific). Peptides were trapped on an Acclaim PepMap 100 (C18, 100 µM x 2 cm) and then separated on an Easy-Spray PepMap RSLC C18 column (75 µM x 50 cm; Thermo Scientific). Data files were searched against ES-associated VSGs using the Mascot Search Engine (Mascot Daemon Version 2.3.2). emPAI scores are proportional to protein content in a protein mixture (15).

SI REFERENCES

1. Alsford S, Kawahara T, Glover L, & Horn D (2005) Tagging a *T. brucei RRNA* locus improves stable transfection efficiency and circumvents inducible expression position effects. *Mol Biochem Parasitol* 144(2):142-148.
2. Glover L*, et al.* (2015) Genome-scale RNAi screens for high-throughput phenotyping in bloodstream-form African trypanosomes. *Nat Protoc* 10(1):106-133.
3. Horn D, Spence C, & Ingram AK (2000) Telomere maintenance and length regulation in *Trypanosoma brucei*. *Embo J* 19(10):2332-2339.
4. Redmond S, Vadivelu J, & Field MC (2003) RNAit: an automated web-based tool for the selection of RNAi targets in *Trypanosoma brucei*. *Mol Biochem Parasitol* 128(1):115-118.
5. Alsford S & Horn D (2008) Single-locus targeting constructs for reliable regulated RNAi and transgene expression in *Trypanosoma brucei*. *Mol Biochem Parasitol* 161(1):76-79.
6. Langmead B & Salzberg SL (2012) Fast gapped-read alignment with Bowtie 2. *Nat Methods* 9(4):357-359.
7. Li H*, et al.* (2009) The Sequence Alignment/Map format and SAMtools. *Bioinformatics* 25(16):2078-2079.
8. Carver T, Harris SR, Berriman M, Parkhill J, & McQuillan JA (2012) Artemis: an integrated platform for visualization and analysis of high-throughput sequence-based experimental data. *Bioinformatics* 28(4):464-469.
9. Hertz-Fowler C*, et al.* (2008) Telomeric expression sites are highly conserved in *Trypanosoma brucei*. *PLoS One* 3(10):e3527.
10. Cross GA, Kim HS, & Wickstead B (2014) Capturing the variant surface glycoprotein repertoire (the VSGnome) of *Trypanosoma brucei* Lister 427. *Mol Biochem Parasitol* 195(1):59-73.
11. Kolev NG, Ramey-Butler K, Cross GA, Ullu E, & Tschudi C (2012) Developmental progression to infectivity in *Trypanosoma brucei* triggered by an RNA-binding protein. *Science* 338(6112):1352-1353.
12. Robinson MD, McCarthy DJ, & Smyth GK (2010) edgeR: a Bioconductor package for differential expression analysis of digital gene expression data. *Bioinformatics* 26(1):139-140.
13. Park JH, Jensen BC, Kifer CT, & Parsons M (2001) A novel nucleolar G-protein conserved in eukaryotes. *J Cell Sci* 114(Pt 1):173-185.
14. Manthri S, Guther ML, Izquierdo L, Acosta-Serrano A, & Ferguson MA (2008) Deletion of the *TbALG3* gene demonstrates site-specific *N*-glycosylation and *N*-glycan processing in *Trypanosoma brucei*. *Glycobiology* 18(5):367-383.
15. Ishihama Y*, et al.* (2005) Exponentially modified protein abundance index (emPAI) for estimation of absolute protein amount in proteomics by the number of sequenced peptides per protein. *Mol Cell Proteomics* 4(9):1265-1272.

A.

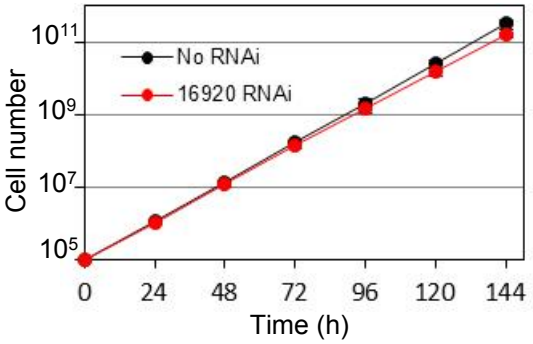

B.

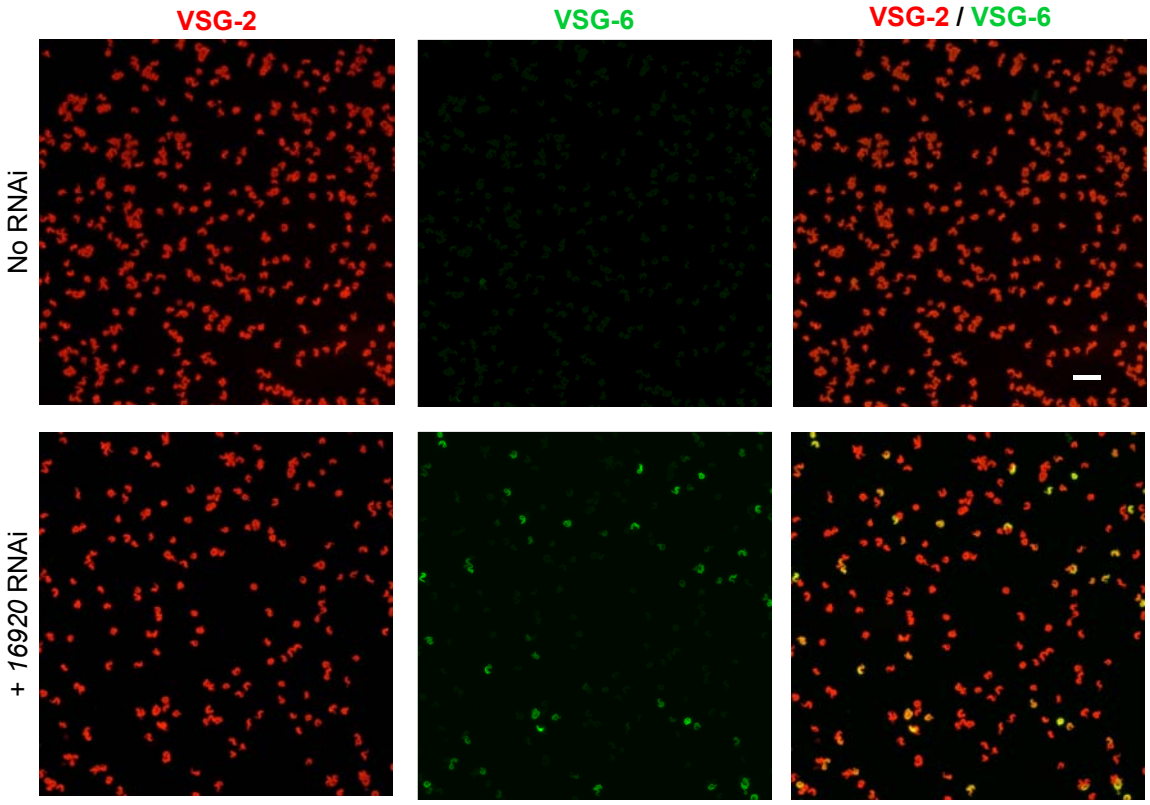

Figure S1. Tb927.11.16920 controls VSG exclusion. (**A**) The growth-curve indicates relative cell-number following Tb927.11.16920 knockdown; data derived from two independent strains. Error bars, SD. (**B**) Immunofluorescence microscopy analysis of VSG-expression after Tb927.11.16920 RNAi (72 h). Cells were stained with both α-VSG-2 and α-VSG-6. Scale bar, 100 μm.

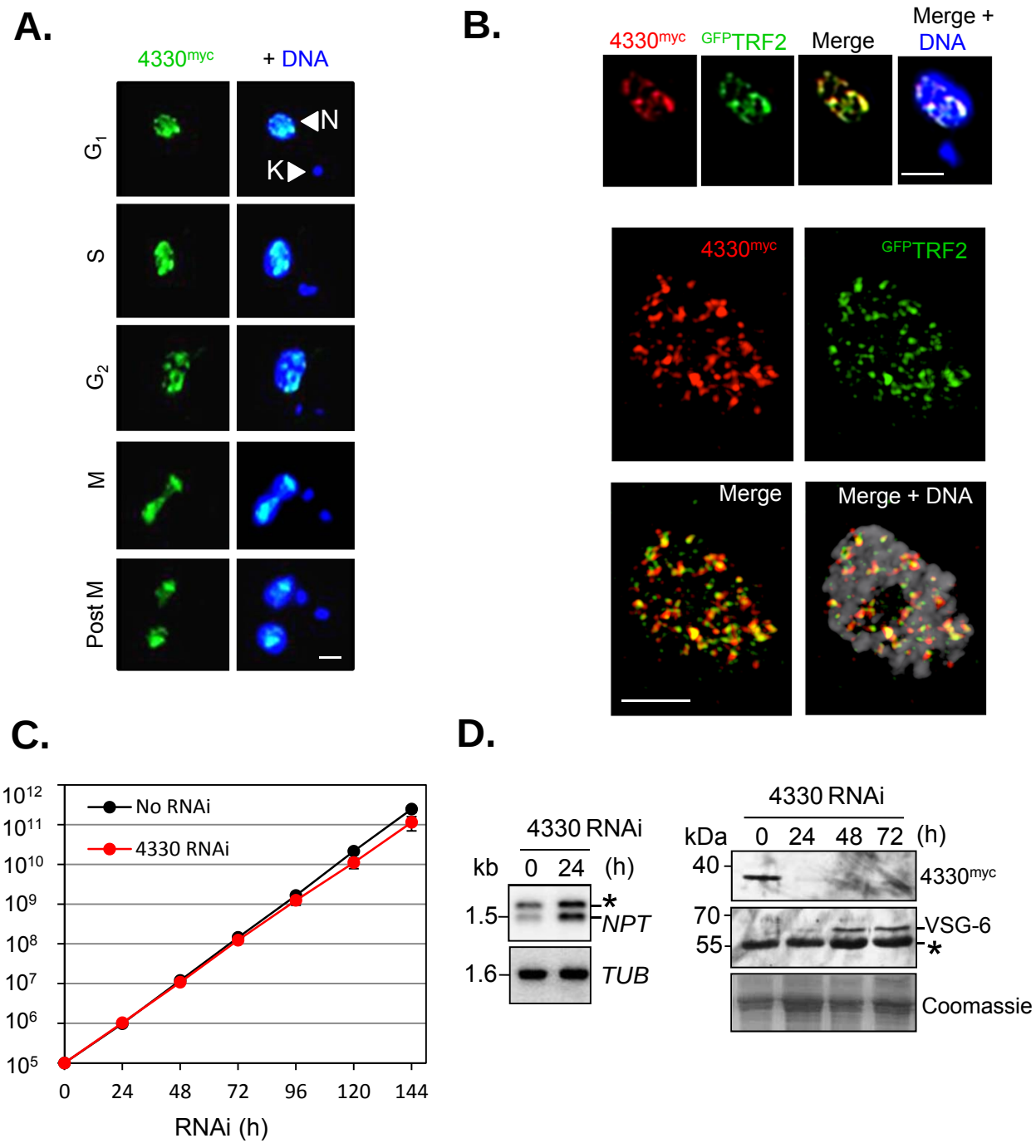

Figure S2. Tb927.6.4330 encodes a telomere-associated protein. (**A**) Immunofluorescence microscopy of Tb927.6.4330^{myc} in bloodstream form *T. brucei*; cell-cycle phases are indicated. DNA was counter-stained with DAPI. N, nucleus; K, kinetoplast (mitochondrial genome). (**B**) Immunofluorescence microscopy of Tb927.6.4330^{myc} and ^{GFP}TRF2. Lower panels, 3D structured illumination projections. Scale bar 2 µm. (**C**) Growth was assessed in two independent Tb927.6.4330 RNAi-knockdown strains. Error bars, SD. (**D**) Subtelomeric *NPT* (left-hand side) and *VSG* derepression (right-hand side) were assessed by RNA and protein blotting, with *TUB* and Coomassie panels as loading controls, respectively. Knockdown was also confirmed by monitoring Tb927.6.4330^{myc} (right-hand side). * indicates a cross-reacting band in each case.

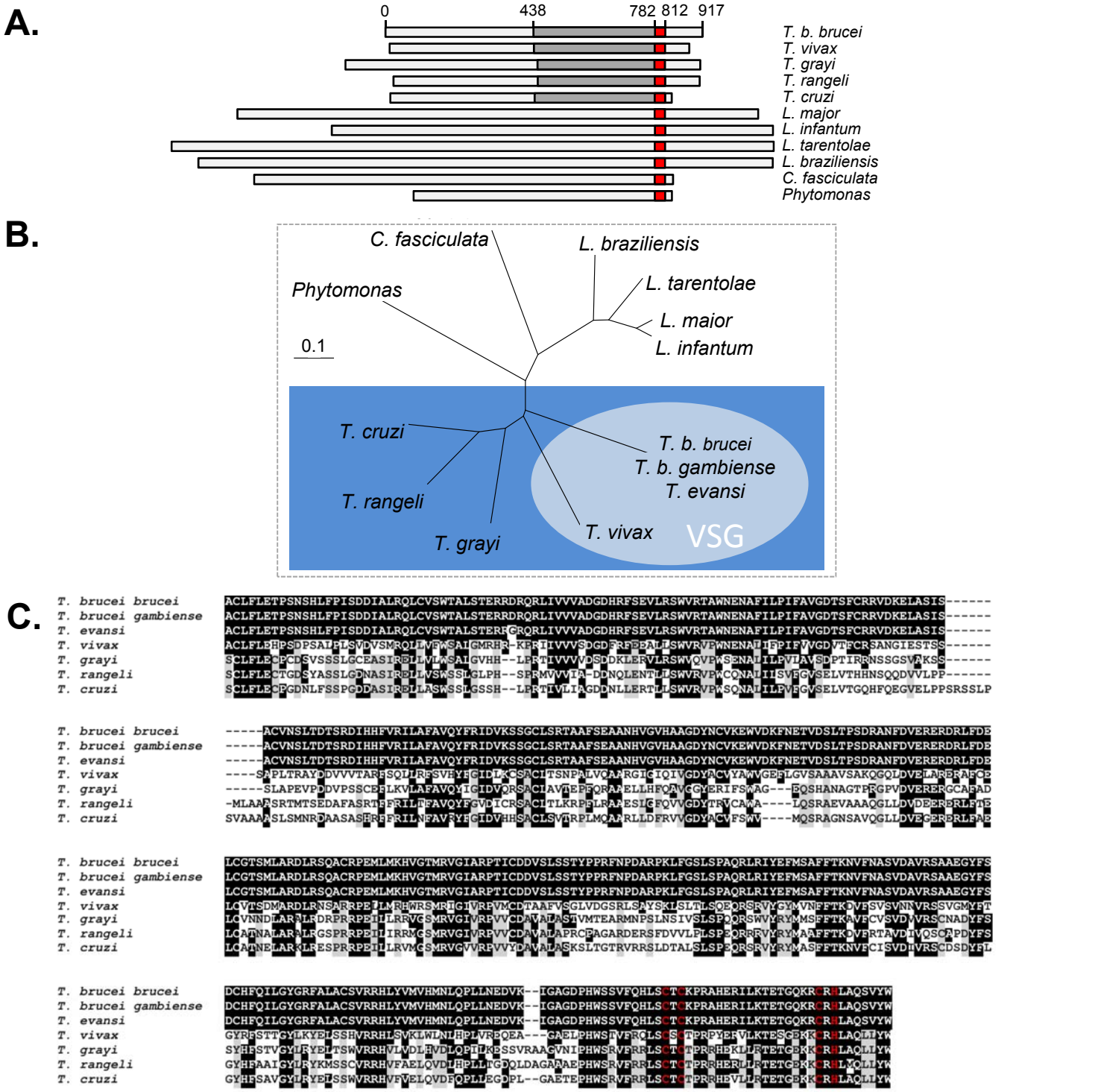

Figure S3. VEX1 Sequence Analysis. (**A**) The schematic shows the predicted VEX1 protein and orthologues encoded by syntenic genes in other trypanosomatids, including parasites of humans and other mammals, crocodiles, plants and insects. The location of the conserved SWIM-type Zn-finger is indicated (red). The grey shaded regions are aligned in C. (**B**) Phylogenetic analysis. The unrooted neighbour-joining tree was generated using clustal 1.8X and TreeView. The blue box indicates sequences aligned in C and the light-blue oval indicates trypanosomes that undergo VSG-based antigenic variation. (**C**) Alignment of a conserved VEX1-region. Residues identical to the *T. b. brucei* sequence are on a black background and other residues shared among >2 other sequences are on a grey background. Key residues of the SWIM-type zinc finger are highlighted (red). The *T. b. brucei* gene (Tb927.11.16920) and the other syntenic gene sequences can be accessed via tritrypdb.org.

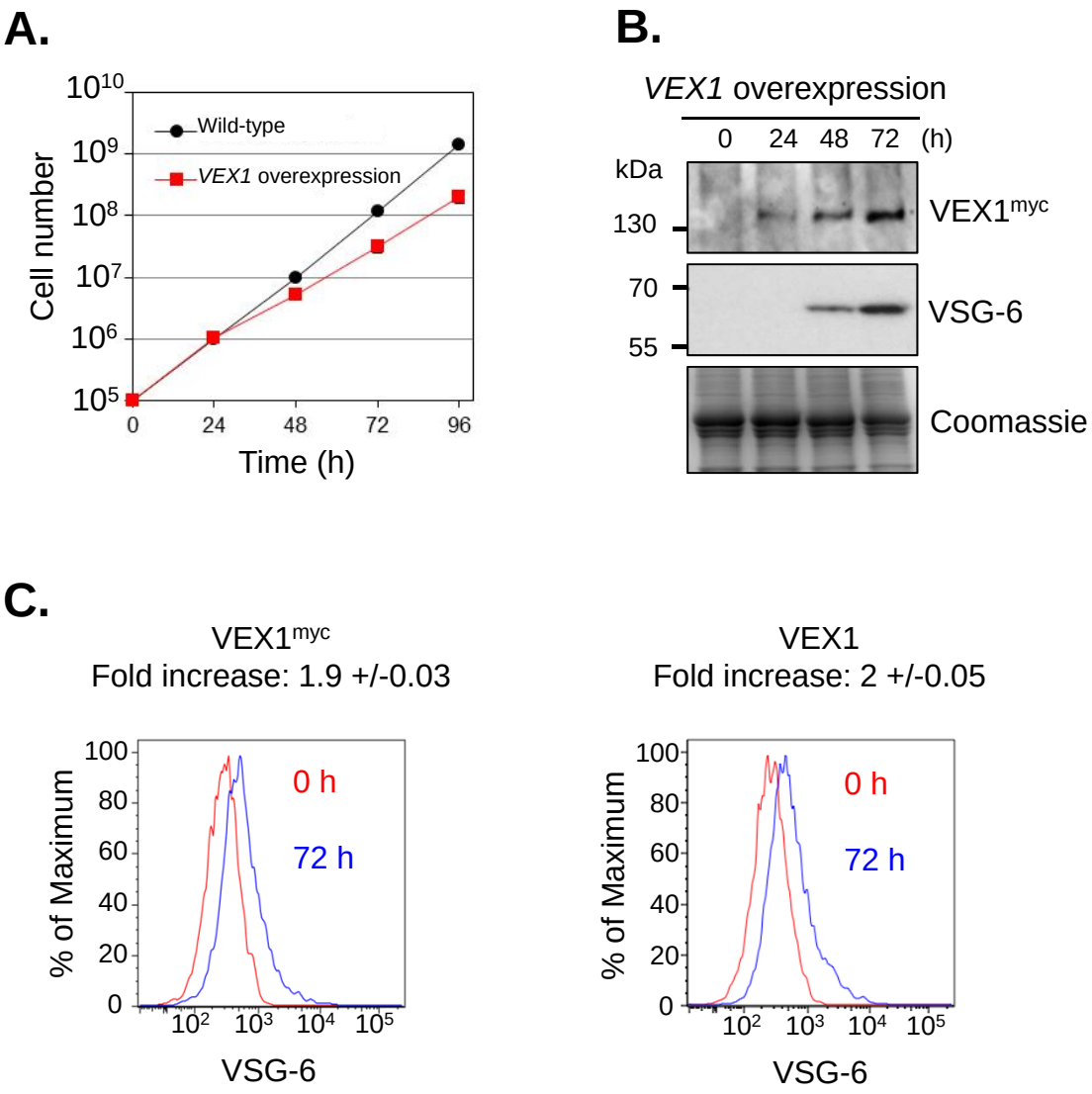

Figure S4. VEX1 overexpression derepresses VSGs. (**A**) The growth-curve indicates relative cell-number following VEX1 overexpression; data derived from two independent strains. Error bars, SD. (**B**) Overexpression of VEX1^{myc} was associated with *VSG-6* derepression as assessed by protein blotting. The Coomassie-stained panel serves as a loading control. (**C**) Flow-cytometry analysis of VSG-6 expression before (red) and after (blue) VEX1 overexpression. Data for myc-tagged VEX1 and native VEX1 are shown. Mean increase in VSG-6 fluorescence intensity is shown +/- SD.

A.

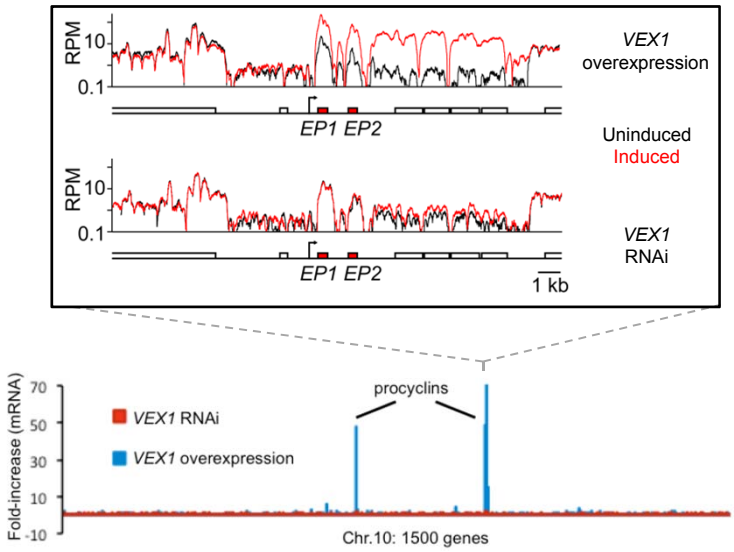

B.

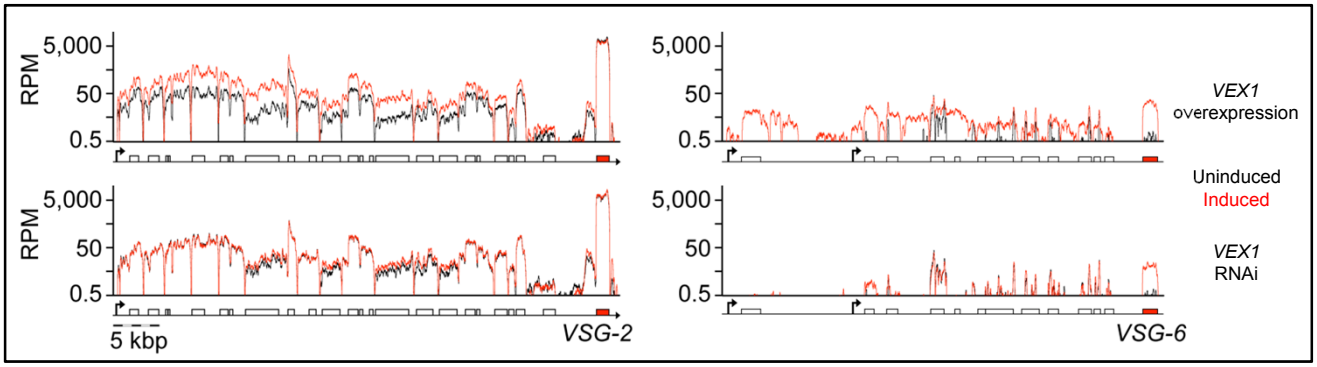

Figure S5. RNA-seq analysis reveals positive and negative control of pol-I loci by VEX1. (**A**) Specific derepression of *procyclin* loci on chr. 10 following *VEX1* overexpression. The upper box shows normalized, single base resolution RNA-seq plots of the *EP1/EP2 procyclin* locus. RPM, reads per million; boxes, protein-coding genes; arrowheads, *procyclin* promoters. (**B**) Specific derepression of *ESAGs* (white boxes) at both active and 'silent' *VSG*-ESs following *VEX1* overexpression. Normalized, single base resolution RNA-seq plots of the active *VSG*-ES (*VSG-2*) and a 'silent' *VSG*-ES (*VSG-6*). Arrowhead above the line, *VSG*-ES promoters.

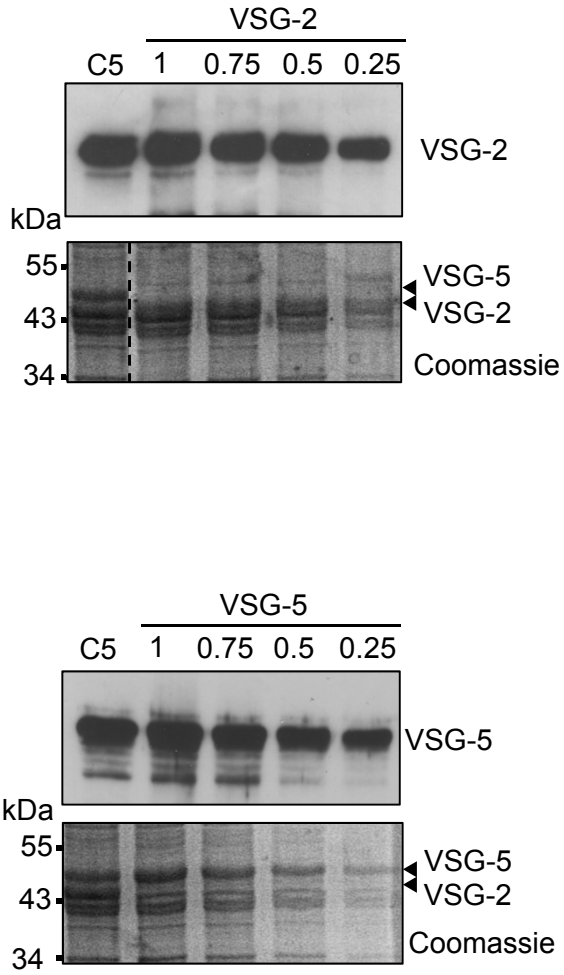

Figure S6. Simultaneous expression of VSG-2 and VSG-5. Western blots probed with a-VSG sera and equivalent Coomassie-stained gels are shown. The top panel shows clone 5 compared to a dilution-series from a wild-type clone expressing VSG-2. The lower panel shows clone 5 compared to a dilution-series from a wild-type clone expressing VSG-5.

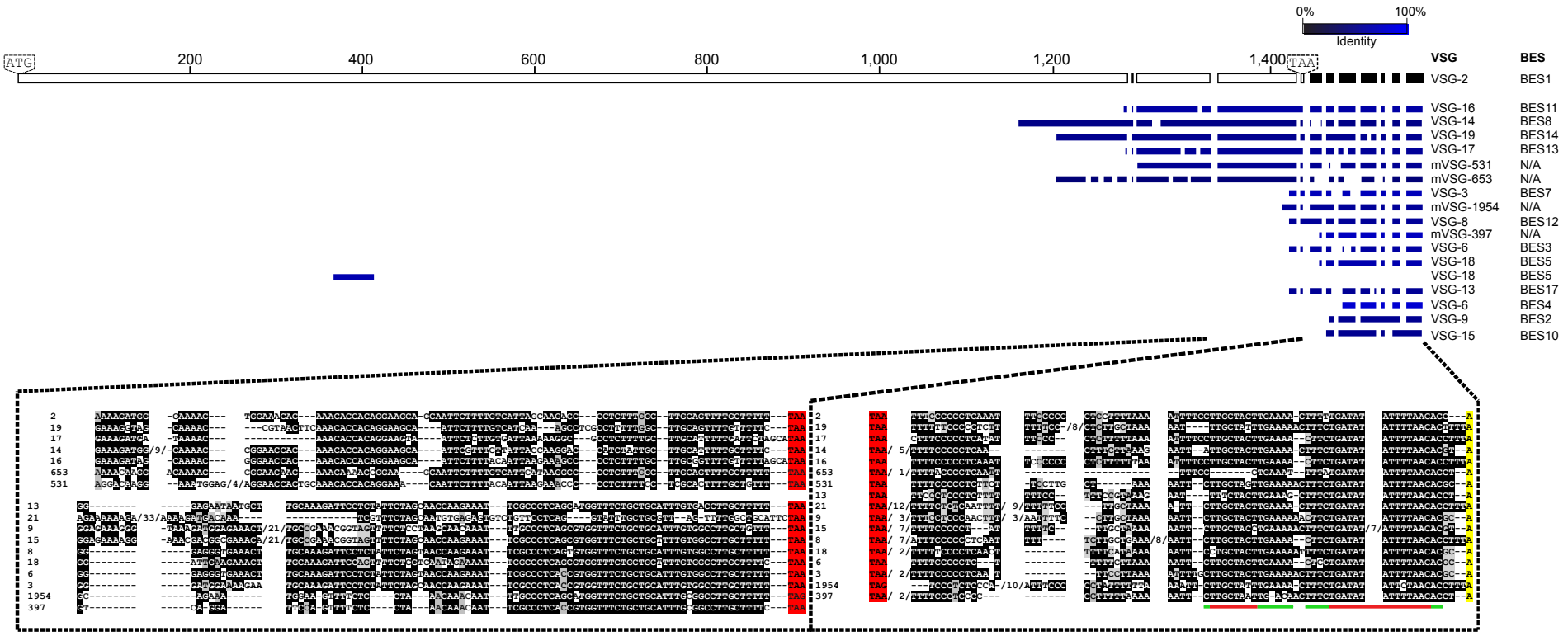

Figure S7. Analysis of *VSG*-associated nucleotide sequences. We analyzed the annotated *VSG*-ES sequences and metacyclic *VSG*-ES sequences from the Lister 427 strain used in this study. Identity ranged from 71-96% over 77 nucleotides in the 3'-UTR and similarity also extended to the *C*-terminal, *VSG*-encoding sequence. The top panel indicates the *VSG-2* query sequence and 'hits' (blue) from BLAST-analysis against a custom database containing the ORF and predicted 3´-UTRs of bloodstream and metacyclic ES-associated *VSG*s. The lower panels show alignments for the regions comprising the majority of hits. The most common bases are on a black background while additional bases shared among >2 additional sequences are on a grey background. Red bars below the alignment indicate a previously identified conserved '8/14mer' while green extended lines indicate that this can be considered a '15/20mer' in the current ES-associated *VSG* cohort.

Gene ID	Protein	Function	Subcellular localisation	Perturbation	Loss of fitness	VSG expression control	VSG switching control	Promoter-adjacent control only	Citation	PMID
Tb927.11.16920	VEX1	Allelic exclusion	Adjacent to ESB	RNAi	Moderate	Y			Current study	Current study
				Overexpression	Moderate	Y				
Tb927.6.4330	-		Telomeres	RNAi	Moderate	Y			Current study	Current study
Tb927.10.7420	BDF2	Ac-Lys binding	Nucleus	Knockout	Moderate	Y			Schulz *et al.*, 2015	26646171
Tb927.11.10070	BDF3	Ac-Lys binding	Nucleus	RNAi	Severe	Y				
Tb927.1.570	DOT1B	Histone methyltransferase	Nucleus	Knockout	Moderate	Y			Janzen *et al.*, 2006	16916638
									Figueiredo *et al.*, 2008	18597556
									Batram *et al.*, 2014	24844706
Tb927.3.5620	FACT (Spt6)	Histone chaperone	*Not determined*	RNAi	Severe	Y			Denninger *et al.*, 2010	20879999
									Denninger & Rudenko, 2014	25266856
Tb927.10.15350	H3var (+J-base)	Histone variant (+DNA modification)	Nucleus	Knockout	None	Y			Reynolds *et al.*, 2016	26796527
Tb927.10.15350	H3var (+J-base)	Histone variant (+DNA modification)	Nucleus	Knockout	None	Y			Schulz *et al.*, 2016	26796638
Tb927.2.1810	ISWI	Chromatin remodelling	Nucleus	RNAi	Severe	Y			Hughes *et al.*, 2007	17431399
									Stanne *et al.*, 2011	21571922
Tb927.7.1770	MCM-BP	Regulator of DNA replication	Nucleus	RNAi	Severe	Y			Kim *et al.*, 2013	23451133
Tb927.10.5450	NLP	ISWI interacting partner	Nucleus	RNAi	Severe	Y			Narayanan *et al.*, 2011	21076155
Tb927.2.4230	NUP1	Nuclear lamin	Nuclear lamina	RNAi	Severe	Y			DuBois *et al.*, 2012	22479148
Tb927.11.7215	ORC	DNA replication	Nucleus	RNAi	Severe	Y			Benmerzouga *et al.*, 2012	23216794
Tb927.4.1620	PIP5K	Inositol Phosphate pathway	Inner plasma membrane	RNAi	Severe	Y			Cestari & Stuart, 2015	25964327
Tb927.11.6270	PIP5Pase		Nucleus/telomeres	RNAi	Severe	Y				
Tb927.11.5970	PLC		Inner plasma membrane	Overexpression	None	Y				
Tb927.11.370	RAP1	Telomeric protein	Telomeres	RNAi	Severe	Y			Yang *et al.*, 2009	19345190
									Pandya *et al.*, 2013	23804762
Tb927.9.11070	Siz1/PIAS1	SUMO E3 ligase	Nucleus	RNAi	Moderate	Y			Lopez-Farfan *et al.*, 2014	25474309
Tb927.5.3210	SUMO	SUMOylation	Primarily nucleus / ESB	RNAi	Severe	Y				
Tb927.3.3940	TDP1	Chromatin structure	Nucleolus + ESB	RNAi	Severe	Y			Narayanan *et al.*, 2013	23361461
									Aresta-Branco *et al.*, 2015	26673706
Tb927.7.6900	SCC1	Sister chromatid cohesion	Nucleus	RNAi	Severe		Y		Landeria *et al.*, 2009	19635842
Tb927.3.1560	TIF2	Telomeric protein	Telomeres	RNAi	Severe		Y		Jehi *et al.*, 2014	24810301
Tb927.10.12850	TRF2	Telomeric protein	Telomeres	RNAi	Severe		Y		Jehi *et al.*, 2014	25313155
Tb927.1.630	ASF1	Histone chaperone	Nucleus	RNAi	Severe			Y	Alsford & Horn, 2012	22941664
Tb927.10.7050	CAF1	Histone chaperone	Nucleus	RNAi	Severe			Y		
Tb927.10.1680	DAC1	Histone Deacetylase	Nucleus	RNAi	Severe			Y	Wang *et al.*, 2010	20624217
Tb927.2.2190	DAC3	Histone Deacetylase	Nucleus	RNAi	Severe			Y		
Tb927.7.1060	FYRP	ISWI interacting partner	*Not determined*	RNAi	Moderate			Y	Stanne *et al.*, 2015	26378228
Tb927.11.1880	Histone H1	Histone	Nucleus	RNAi	Moderate			Y	Povelones *et al.*, 2012	23133390
									Pena *et al.*, 2014	24946224
Tb927.1.2430	Histone H3	Histone	Nucleus	RNAi	Severe			Y	Alsford & Horn, 2012	22941664
Tb927.11.10330	RCCP	ISWI interacting partner	*Not determined*	RNAi	Moderate			Y	Stanne *et al.*, 2015	26378228

Table S1. Genes Linked to *VSG*-ES Transcription Control in Bloodstream-Form *T. brucei.*

VSG	Wild-type				*VEX1* overexpression				*VEX1* knockdown			
	Score	Significant matches	Significant sequences	emPAI	Score	Significant matches	Significant sequences	emPAI	Score	Significant matches	Significant sequences	emPAI
2	10473	351	38	29.94	7117	249	40	40.6	9457	336	40	48.68
6	64	2	1	0.05	804	28	11	0.88	1050	31	13	0.98
8	0	0	0	0	388	15	10	0.82	817	30	16	1.77
11	0	0	0	0	525	12	5	0.46	276	6	3	0.24
531	167	4	1	0.06	542	9	6	0.42	346	6	4	0.26
18	0	0	0	0	478	11	4	0.38	300	5	3	0.24
397	0	0	0	0	233	9	4	0.25	69	4	3	0.18
15	0	0	0	0	70	3	3	0.17	96	4	3	0.17
653	0	0	0	0	97	5	2	0.13	56	2	2	0.13
1954	0	0	0	0	238	4	1	0.12	139	3	2	0.18
3	0	0	0	0	121	3	1	0.06	23	1	1	0.06
13	0	0	0	0	93	2	1	0.06	81	2	1	0.06
21	0	0	0	0	74	2	1	0.06	0	0	0	0

Table S2. VSG Quantitative Mass-Spectrometry Data. emPAI, exponentially modified Protein Abundance Index.